Evidence for an Electric-Dipole Active Continuum Band of Spin Excitations in Multiferroic $TbMnO_3$

Y. Takahashi,[1] N. Kida,[1] Y. Yamasaki,[2] J. Fujioka,[2] T. Arima,[3] R. Shimano,[1,4] S. Miyahara,[1] M. Mochizuki,[1] N. Furukawa,[1,5] and Y. Tokura[1,2,6]

[1]*Multiferroics Project, ERATO, Japan Science and Technology Agency (JST), Japan c/o Department of Applied Physics, The University of Tokyo, Tokyo 113-8656, Japan*

[2]*Department of Applied Physics, The University of Tokyo, Tokyo 113-8656, Japan*

[3]*Instisute of Multidisciplinary Research for Advanced Materials, Tohoku University, Sendai 980-8577, Japan*

[4]*Department of Physics, The University of Tokyo, Tokyo 113-0033, Japan*

[5]*Department of Physics and Mathematics, Aoyama Gakuin University, Sagamihara, Kanagawa 229-8558, Japan*

[6]*Cross-Correlated Material Research Group (CMRG), FRS, RIKEN, Wako, Saitama 351-0198, Japan*

(Received 20 June 2008; revised manuscript received 5 August 2008; published 27 October 2008)

The wide range optical spectra on a multiferroic prototype $TbMnO_3$ have been investigated to clarify the origin of spin excitations observed in the far-infrared region. We elucidate the full band structure, whose high energy edge (133 cm^{-1}) exactly corresponds to twice of the highest-lying magnon energy. Thus the origin of this absorption band is clearly assigned to two-magnon excitation driven by the electric field of light. There is an overlap between the two-magnon and phonon energy ranges, where the strong coupling between them is manifested by the frequency shift and transfer of oscillator strength of the phonon mode.

DOI: 10.1103/PhysRevLett.101.187201 PACS numbers: 75.80.+q, 75.40.Gb, 76.50.+g

Multiferroics, in which electric and magnetic properties are cross-correlated, have attracted much attention in recent years because of their novel magnetoelectric phenomena as well as possible applications [1]. Substantial efforts have been dedicated to the research on controlling the electric polarization and magnetization with external magnetic and electric field, respectively. It is also expected that the strong coupling may appear not only in static properties but also in dynamical responses, such as electrically driven magnetic excitations. One of the major origins of magnetically induced electric polarization is the inverse of the Dzyaloshinski-Moriya interaction [2,3]. In this mechanism, a transverse-spiral spin structure yields macroscopic polarization (P_s), which is given by the sum of local polarization generated by interacting neighboring spins S_i and S_j; $P_{ij} \propto e_{ij} \times (S_i \times S_j)$, with the connecting unit vector e_{ij}, as shown in Fig. 1(a). The spin spiral plane and sign of helicity determine the direction of P_s. Orthorhombic perovskite $RMnO_3$ with rare earth $R =$ Tb, Dy, Gd and $Eu_{1-x}Y_x$ are prototypes of such multiferroics with the spiral spin structure [4–10]. In $TbMnO_3$, for example, the collinear spin order of Mn ions sets in at Néel temperature T_N of 41 K and the ferroelectric phase appears in the bc-spiral spin state with the magnetic q vector along the b axis below 28 K, where the P_s is parallel to the c axis [4,6]. The sign change of helicity upon the reversal of the P_s was directly observed by a spin-polarized neutron scattering study on $TbMnO_3$ [8].

Under the coupling between magnetism and electricity, the collective excitation is anticipated to exist. The collective excitation directly reflecting the inverse Dzyaloshinski-Moriya mechanism is the rotation mode of the spiral plane that is driven by electrical field [11]. This $k = 0$ magnon mode should be active for the light E vector perpendicular to the spin spiral plane. The first experimental attempt to explore such excitations was reported by Pimenov *et al.* in $TbMnO_3$ and $GdMnO_3$ [12], where they observed the growth of the absorption band in $E^\omega \parallel a$ below 40 cm^{-1} in accordance with the spin order and called the excitation *electromagnon*. The results for $Eu_{1-x}Y_xMnO_3$ were also reported in Refs. [13,14], in which the growth of the absorption band in $E^\omega \parallel a$ configuration was also observed. On the basis of the theoretical prediction mentioned above, the polarization selection rule for the electromagnon, the absorption band in $Eu_{1-x}Y_xMnO_3$ with $P_s \parallel a$ should be $E^\omega \parallel c$. This discrepancy suggests that the origin of the absorption may be another kind of magnetic excitations. Recently, Kida *et al.* reported detailed temperature and magnetic field dependence of $DyMnO_3$ by THz time-domain spectroscopy, and observed that the absorption band for $E^\omega \parallel a$ is essentially sustained even in the magnetic-field-induced $P_s \parallel a$ phase [15]. One possible candidate of the origin of absorption band to explain the continuumlike excitation is the infrared-active two-magnon (2M) excitations (or electro-two-magnons) [13,15]. To clarify the origin of this far-infrared absorption, a comparison between the complete optical spectra and the magnon band structure would be necessary. As for $TbMnO_3$, the inelastic neutron measurement was recently reported by Senff *et al.* [16] to determine the low-lying magnon dispersion up to 65 cm^{-1} [Fig. 1(b)]. Thus the elucidation of the full absorption

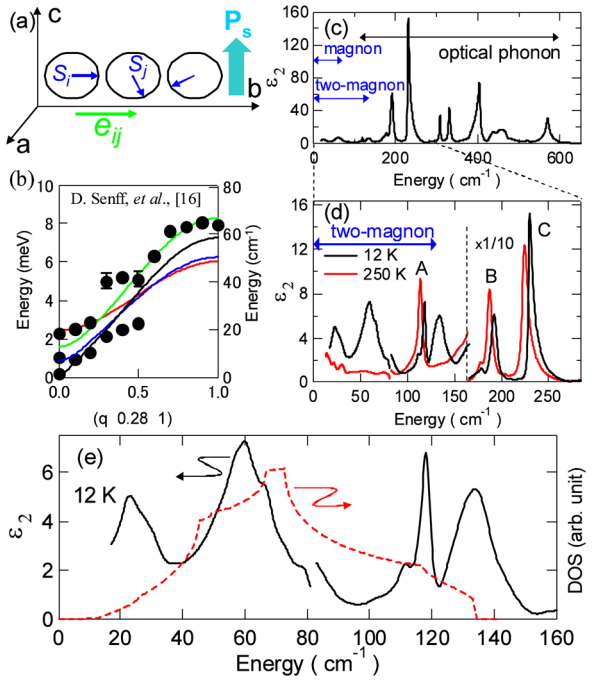

FIG. 1 (color online). (a) The schematic of the spin structure and direction of the spontaneous polarization in the bc-plane transverse-spiral (cycloidal) spin state of $TbMnO_3$ in the orthorhombic setting. (b) The magnon dispersion reproduced from Ref [16]. Solid lines represent the dispersion calculated by the linear spin wave theory on the bc-spiral state with use of spin exchange interaction parameters; $J_1 = -0.85$ meV, $J_2 = +0.68$ meV, and $J_c = +1.28$ meV (see text).(c) The ϵ_2 spectrum with $E^\omega \parallel a$ at 12 K. The energy region of the magnon, the 2M excitation, and optical phonon are indicated by arrows. (d) The ϵ_2 spectra at 12 and 250 K below 290 cm^{-1}, where the magnetic excitation and the lower-lying optical phonon modes are located. The phonon modes in this energy range are denoted as A, B, and C. (e) The ϵ_2 spectrum at 12 K and for $E^\omega \parallel a$ of the 2M band and the lowest optical phonon mode, where the tail of the phonon B is subtracted. Dashed line represents the DOS of the 2M excitation obtained by the linear spin wave theory (see text).

band structure for $TbMnO_3$ as well as its temperature and light polarization dependence may provide a clue to the puzzling infrared-active spin excitation in those multiferroic perovskite manganites.

Another interest is in the possible interplay between such spin excitations and phonons. In $GdMnO_3$, changes of frequency and strength in the lowest optical phonon mode were reported by applying magnetic field [17]. The coupling with the lowest optical phonon mode was also reported in $Eu_{0.75}Y_{0.25}MnO_3$, where the transfer of oscillator strength between the lowest phonon and spin excitation was observed [13]. To understand the coupling with phonon, an accurate measurement in a wider energy range will be required. Here we conducted from THz to ultraviolet spectroscopy to search for the possible signature of the coupling of the dipole-active spin excitation with the phononic and electronic excitations. We could clarify a full spectrum shape of magnetic excitation, which was unambiguously assigned to the 2M excitation band. The coupling with the lowest optical phonon mode, which is buried in the 2M excitation continuum, was also investigated in detail.

A single crystal of $TbMnO_3$ was grown by a floating-zone method in a flow of Ar gas. We performed THz time-domain spectroscopy in transmittance configuration to determine both of the real and imaginary parts of the complex dielectric constant from 13 to 80 cm^{-1}. The THz wave was generated by the optical rectification of ultrashort pulses in a ZnTe(110) crystal and detected by a dipole antenna [18]. We conducted reflection and transmission FTIR measurements from 80 to 650 cm^{-1}, where the 22 μm-thick sample was used for the transmission measurement. We determined the complex dielectric constant using reflectance and transmittance data in an energy range from 83 to 180 cm^{-1}. Above 180 cm^{-1}, we used Kramers-Kronig transformation to obtain the complex dielectric constant. The reflection spectra for the Kramers-Kronig transformation were obtained up to ultraviolet region (40 000 cm^{-1}).

Figure 1(c) shows the imaginary part of the dielectric constant, ϵ_2, between 13 and 650 cm^{-1}, which corresponds to optical phonon and magnon energy range as indicated in the figure, in $E^\omega \parallel a$ configuration at 12 K. Several phonon modes due to the orthorhombic distortion are observed. In Fig. 1(d), we focus on the low-energy region including magnetic excitations and three low-energy phonons, where the coupling between magnetic and electric excitations is expected to show up clearly. Three phonon modes, 112 (A), 190 (B) and 225 cm^{-1} (C), all the so-called external modes as dominated by the character of Tb-O vibration, are observed at 250 K as shown in Fig. 1(d). At 12 K, where the ferroelectric and bc-plane spin spiral phase emerge, the development of broad continuumlike absorption band, composed of broad peak structures at 20, 55, and 133 cm^{-1}, is clearly observed. Since the absorption band expands up to 150 cm^{-1}, this band cannot be explained by the single magnon Goldstone mode at $k = 0$ which is expected at 10–20 cm^{-1} [see Fig. 1(b)]. The highest-energy peak (133 cm^{-1}) of this broad band precisely corresponds to the upper edge of the 2M energy range, i.e., twice the highest one-magnon energy, 67 cm$^{-1} \times 2 = 134$ cm^{-1}. Thus it is quite reasonable to assign the origin of the broad absorption band to the 2M excitation. We show the complete band structure including the lowest phonon A in Fig. 1(e), where the contribution of phonon B is subtracted from the ϵ_2 spectrum by a fitting procedure using Lorentz function. To calculate the density of states (DOS) of the 2M band, we have fitted the experimentally observed magnon dispersion in Ref. [16] by using the linear spin wave theory with the spin exchange interaction parameters, $J_1(ab\,\text{plane}) = -0.85$ meV, $J_2(ab\,\text{plane}) = +0.68$ meV and $J_c(c\,\text{axis}) = +1.28$ meV, as well as of the single-ion anisotropy term ($D = 0.13$ meV) [solid lines in Fig. 1(b)]. We have confirmed that this set of parameters can repro-

duce the bc-spiral spin state [19]. The 2M DOS, i.e., twice the energy scale of the one-magnon DOS, calculated with use of these obtained parameters is shown with a dashed line in Fig. 1(e). The energy ranges of the two spectra coincide with each other, while the spectral shapes are considerably different. The midpeak around 55 cm^{-1} perhaps reflects the 2M DOS singularity, but why the lower and upper edges of the 2M band can show up strongly in the optical absorption spectrum is left to be theoretically elucidated.

Figure 2 shows the ϵ_2 spectra in all the crystallographically independent light polarization configurations. The temperatures of 250, 30, and 12 K correspond to the paramagnetic, collinear sinusoidal and bc-spiral phase, respectively. The obvious enhancement of ϵ_2 is observed for $E^\omega \parallel a$ in the bc-spiral phase and this behavior is consistent with recent observations for $DyMnO_3$ [15], $TbMnO_3$ [12], $GdMnO_3$ [17] and $Eu_{1-x}Y_xMnO_3$ [13,14]. The lowest-energy peak locating around 20 cm^{-1} has already been reported by Pimenov *et al.* [12]. In $E^\omega \parallel b$, $H^\omega \parallel c$ configuration, the tiny peak is identified around 20 cm^{-1} at 12 K. Since this absorption peak is active only for $H^\omega \parallel c$ (not observed in $E^\omega \parallel b$, $H^\omega \parallel a$ configuration) and the peak energy just corresponds to that of one magnon at $k = 0$ [16], it is assigned to the conventional antiferromagnetic (one-magnon) resonance. From these polarization dependencies, we can conclude that the intense absorption band arises only for $E^\omega \parallel a$, irrespective of the polarization direction of H^ω, apart from the weak one-magnon absorption [20].

Figure 3 shows the temperature (T) dependence of ϵ_2 spectra up to 180 cm^{-1} for $E^\omega \parallel a$. Below 80 cm^{-1} (indicated as the region I), a flat broad band is discerned in the collinear sinusoidal phase at 30 and 40 K. In the ferroelectric (bc-spiral) phase below 28 K, the two-peak structure appears in this low-energy region (20-80 cm^{-1}) and their intensity develops rapidly. In contrast, the upper edge of the 2M band around 130 cm^{-1} (the region III) steadily grows in intensity even from the paramagnetic phase (80 K). In the energy range between 93 and 122 cm^{-1} (the region II), where the spectra are dominated by the phonon mode A, the spectral intensity and peak position show significant T dependence. Hardening of the mode frequency and sharp decreasing of the intensity with decreasing T are clearly observed. These tendencies suggest a strong coupling of this phonon mode with the 2M excitation.

To be more quantitative, we introduce the integrated spectral weight per Mn site, $N_{\rm eff}$, as given by

$$N_{\rm eff} = \frac{2m_0 V}{\pi e^2} \int_{\omega 1}^{\omega 2} \omega' Im[\epsilon(\omega')] d\omega', \qquad (1)$$

where m_0, e, and V are the free electron mass, the electric charge and the unit-cell volume, respectively. We define $\Delta N_{\rm eff}$ as $\Delta N_{\rm eff} = N_{\rm eff}(T) - N_{\rm eff}(250\ {\rm K})$. We divide the 2M continuum band into the three energy ranges; I, II and III as shown in Fig. 3. Figure 4(a) shows the T dependence of $\Delta N_{\rm eff}$ in each energy region. The $\Delta N_{\rm eff}$ shows slight decline below 250 K in all the regions due to the change of the absorption tail arising from the higher-energy phonons. This variation is, however, negligible as compared with substantial changes observed at low T. With decreasing T, the 2M intensity in the highest-energy region III increases from 150 K, a much higher T than T_N (41 K). In contrast, the low-energy side (the region I) of the 2M band shows rapid build-up from T_N and the intensity-increasing rate becomes higher in the bc-spiral phase as shown in Fig. 4(b). This large energy-region dependence of development of 2M band may be ascribed to the anisotropic development of spin short-range order above T_N. The short-range order enables the 2M generation with large wave number near the zone edge. In $TbMnO_3$, the exchange interaction along the a and c axes are simply ferro- and antiferromagnetic, contrary to the frustrated b axis [21] and it is possible that the short-range order along the a and c axes evolve at first even well above T_N. On the other

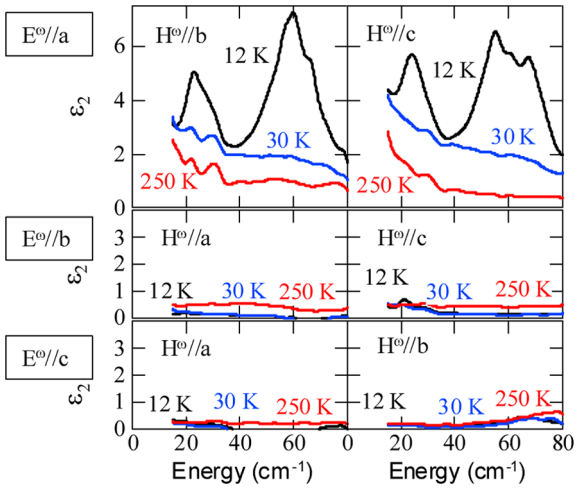

FIG. 2 (color online). The ϵ_2 spectra in all the polarization (E^ω, H^ω) configurations of light, measured at 12, 30, 250 K. E^ω and H^ω represent electric and magnetic fields of light.

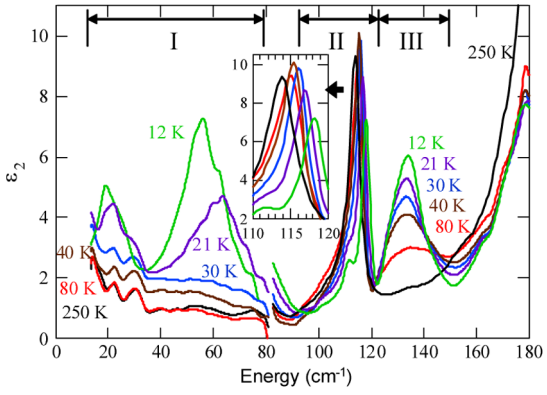

FIG. 3 (color online). Temperature dependence of the ϵ_2 spectra in $E^\omega \parallel a$. Three energy ranges are indicated as I, II, and III. The inset shows the detailed change of the phonon mode A between 110 and 120 cm^{-1}.

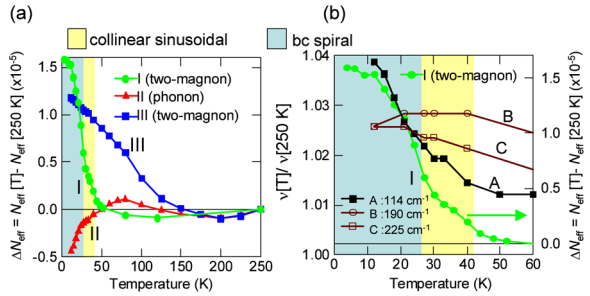

FIG. 4 (color online). (a) Temperature variation of the spectral weight (N_{eff}; see text for the definition) in the respective energy regions, I, II and III (see Fig. 3). ΔN_{eff} is defined as the difference from the N_{eff} value at 250 K. (b) The temperature dependence of the phonon mode frequencies normalized by the respective values at 250 K, where A, B, and C indicates the phonon modes as defined in Fig. 1(d). The ΔN_{eff} in the energy region I (the lower-energy region of the 2M band) is also shown.

hand, it is reasonable that the development of the 2M band in the low-energy region (I) shows strong correlation with the formation of the long-range order, because the response of low-energy region reflects the magnon generation with small wave number.

The next issue we should consider is a mechanism of coupling between the 2M excitation and phonon. As mentioned above, the phonon at 113 cm^{-1} (A), located within the continuum of the 2M band, may give a good clue to the coupling mechanism. The ΔN_{eff} of the phonon A, whose energy range is indicated as the region II in Fig. 3, is shown in Fig. 4(a). The small minimum around 200 K is again attributed to the decrease of the low-energy tail of the higher-lying phonon modes, while the slight increase is seen below 150 K with decreasing T. The latter structure originates from the tail of the 2M band in the high-energy region III, because the development of its intensity is similar to that of the 2M band. Aside from these trivial T-variations, the ΔN_{eff} in the region II shows a decrease below 80 K and then a steep decrease in the bc-spiral phase. This result indicates that the phonon A is strongly correlated with the 2M excitation in region I, where the long-range cycloidal order is evolved with the growth of P_s and a part (about 30%) of the oscillator strength of the phonon mode A is transferred to that of the 2M excitation.

Another evidence for the coupling between the phonon mode A and the 2M continuum can be seen in the shift of the peak position of A as shown in Fig. 4(b). The T-dependent blue shift of the higher-lying phonon modes B and C with lowering T are small and almost terminated below T_N. However the mode A shows increase of frequency in undergoing the transition to the collinear sinusoidal phase and even steeper increase in the bc-spiral phase; the T variation is similar to the ΔN_{eff} in the region I. These results indicate that lowest-lying phonon mode A locating inside the 2M continuum shows a particularly strong coupling with the 2M excitation via the Fano-like resonance. Nevertheless, the increase of the oscillator strength in the region I and III at 12 K is 6 times as large as the decrease of that of II-region (the phonon mode A). In the light of the sum rule, the 2M spectral weight comes not only from the nearby optical phonon (like the mode A), but also from higher-lying phonon modes and/or the other electronic excitations.

To conclude, we investigated the origin of the far-infrared absorption in multiferroic $TbMnO_3$, where the electrically driven spin excitation has been observed for $E^{\omega} \parallel a$. We elucidated the complete structure of the infrared-active spin excitation band, whose full width is over 130 cm^{-1}, and showed that the energy range of the absorption band exactly corresponds to that expected for the two-magnon (2M) excitation. The phonon-2M coupling is conspicuous for the lowest phonon mode lying within the 2M continuum, as seen in its frequency shift and decrease of oscillator strength with decreasing T. The present results on this representative multiferroic will give a clue to the microscopic origin of the strongly dipole-active 2M excitation.

This work was in part supported by Grant-In-Aids for Scientific Research (16076205 and 20340086) from the Ministry of Education, Culture, Sports and Technology (MEXT), Japan.

[1] Y. Tokura, Science **312**, 1481 (2006); W. Eerenstein, N. D. Mathur, and J. F. Scott, Nature (London) **442**, 759 (2006); S-W. Cheong and M. Mostovoy, Nature Mater. **6**, 13 (2007).
[2] H. Katsura, N. Nagaosa, and A. V. Balatsky, Phys. Rev. Lett. **95**, 057205 (2005).
[3] I. A. Sergienko and E. Dagotto, Phys. Rev. B **73**, 094434 (2006).
[4] T. Kimura *et al.*, Nature (London) **426**, 55 (2003).
[5] T. Goto, T. Kimura, G. Lawes, A. P. Ramirez, and Y. Tokura, Phys. Rev. Lett. **92**, 257201 (2004).
[6] T. Kimura, G. Lawes, T. Goto, Y. Tokura, and A. P. Ramirez, Phys. Rev. B **71**, 224425 (2005).
[7] M. Kenzelmann *et al.*, Phys. Rev. Lett. **95**, 087206 (2005).
[8] Y. Yamasaki *et al.*, Phys. Rev. Lett. **98**, 147204 (2007).
[9] J. Hemberger *et al.*, Phys. Rev. B **75**, 035118 (2007).
[10] Y. Yamasaki *et al.*, Phys. Rev. B **76**, 184418 (2007).
[11] H. Katsura, A. V. Balatsky, and N. Nagaosa, Phys. Rev. Lett. **98**, 027203 (2007).
[12] A. Pimenov *et al.*, Nature Phys. **2**, 97 (2006).
[13] R. Valdés Aguilar *et al.*, Phys. Rev. B **76**, 060404(R) (2007).
[14] A. Pimenov *et al.*, Phys. Rev. B **77**, 014438 (2008).
[15] N. Kida *et al.*, Phys. Rev. B **78**, 104414 (2008).
[16] D. Senff *et al.*, Phys. Rev. Lett. **98**, 137206 (2007).
[17] A. Pimenov *et al.*, Phys. Rev. B **74**, 100403(R) (2006).
[18] B. Ferguson and X. -C. Zhang, Nature Mater. **1**, 26 (2002).
[19] M. Mochizuki and N. Furukawa (unpublished).
[20] With the decoupling procedure between $\epsilon(\omega)$ and $\mu(\omega)$ in Ref. [15], we deduced the peak magnitude of $\mu_2 = 0.04$ for this 20 cm^{-1} antiferromagnetic resonance.
[21] T. Kimura *et al.*, Phys. Rev. B **68**, 060403(R) (2003).